MECSOL 2022 - Proceedings of the 8th International Symposium on Solid Mechanics
M.L. Bittencourt, J. Labaki, L.C.M. Vieira Jr. and E. Mesquita (Editors), Campinas SP, Brazil, October 17th to 19th, 2022

Optimization of Vibration Band Gaps in Damped Elastic Metamaterials

Rubens G. Salsa Jr.[1], Thiago de P. Sales[2] and Domingos A. Rade[2]

[1] Federal University of Rio Grande do Norte, Department of Mechanical Engineering, Natal, RN 59078-970, Brazil
[2] Aeronautics Institute of Technology, Division of Mechanical Engineering, São José dos Campos, SP 12228-900, Brazil

Abstract. In structural dynamics, the band gap phenomena have been extensively researched as means to reduce vibration transmission in elastic metamaterials. For non-dissipative structures, band gaps can be obtained from the dispersion relation and they are associated with frequency ranges where no propagating wave modes exist. The presence of damping makes this approach inconvenient to determine band gaps because all wave modes exhibit attenuation. Since some level of damping is unavoidable in real structures, it is necessary to include dissipation to improve the predictability of the mathematical models. In this regard, the main objective of this work is to obtain an optimal design of a damped three-dimensional elastic meta-structure. This meta-structure was modeled by the finite element method and wave modes were obtained by taking into account Floquet-Bloch boundary conditions. Band gaps were identified with an evanescence index and the dependence of the band gaps of the investigated lattice structure on design parameters was duly analyzed. Throughout the text, the main differences in optimization procedure between a damped and undamped structure are highlighted. It has been verified that the optimal damped meta-structure has wider range of attenuation than the undamped optimal one, but with decreased peak of attenuation. At last, the optimization procedure was validated numerically for a finite structure, which demonstrated reduced transmissibility of bending, longitudinal and torsional motions. This demonstrates the potential utility of this elastic meta-structure in diverse applications requiring vibration suppression.
Keywords: elastic metamaterials, periodic structures, band gaps, phonic crystals, optimization, damping

INTRODUCTION

Metamaterials consist of structures constructed from a periodic repetition of identical substructures or unit cells, engineered to exhibit properties that are generally viewed to go beyond what one expects to find in naturally occurring or conventional materials. One of the most important features of metamaterials is the possible existence of frequency ranges, known as band gaps, within which the propagation of elastic waves in the structure is prohibited or only evanescent waves with spatial decay exist (Vasileiadis et al., 2021), rendering them appealing to a vast range of engineering applications demanding vibration suppression or mitigation, offering advantages when compared to the cost of standard high-mass structures. The attenuation phenomenon, named Bragg scattering, occurs when the wavelengths of traveling waves become twice the length of the unit cells, so that transmitted and reflected waves within the periodic media undergo destructive interference (Vasileiadis et al., 2021). Because of the dependence on wavelength, which in turn is related to structural stiffness, Bragg band gaps tend to occur at relatively high frequencies in many engineering structures.

With the purpose of obtaining band gaps in lower frequency ranges for practically realizable engineering systems, researchers have often resorted to elastic meta-structures. They consist of metamaterial structures embedded with local resonances and the goal is that each resonator act akin to a dynamic vibration absorber. Resonant-type band gaps have been extensively studied recently and they show potential for tunability of internal resonances, which can leverage the local resonance mechanism between the unit cell and the auxiliary oscillators to ensure a variety of functional improvements, evidencing that elastic meta-structures can provide transmissibility reduction of elastic waves, with potential use where vibration isolation is an essential property.

While research on elastic meta-structures mostly focuses on obtaining dispersion relations and analyzing the effect of local resonator design parameters on band gap width and location, a challenging issue arises when obtaining new configurations that result in wider band gaps in lower frequency ranges. Because of the nontrivial interplay between different components in complex engineering systems, this task has been tackled with the systematic implementation of optimization procedures to determine the optimal design of metamaterials and local resonators for some types of structures. Jung et al. (2020) used a topology optimization method for designing a local resonator in order to tailor flexural band gaps in plate structures. Bacigalupo et al. (2017) combined anti-chiral lattice structure with inertial resonators, and designed the number, arrangements, and material properties of the resonators to improve band gap properties using a nonlinear optimization algorithm. Later, Bacigalupo et al. (2019) successfully utilized machine-learning techniques to the

spectral optimization of a tetrachiral metamaterial. Dal Poggetto et al. (2019) obtained an optimal resonator distribution in a tall building to maximize the width of the formed band gap for a given beam and frequency range of interest using the GlobalSearch function from Matlab. A sequential quadratic programming algorithm was used to solve a constrained nonlinear optimization problem by Dal Poggetto et al. (2021) and Dal Poggetto and Arruda (2021) to obtain solutions that maximize an objective function capable of yielding low-frequency band gaps in a plate and to design spider web-inspired single-phase phononic crystals through selective variation of thread radii and the addition of point masses, respectively. Recently, Salsa Jr et al. (2021) used an evolutionary algorithm to optimize the local resonators of a three-dimensional meta-structure to obtain lower and wider band gaps when compared to the resonator-free counterpart.

A common characteristic in these works is that models for metamaterials under consideration have no damping mechanism. When damping is considered, all frequency dependent wave numbers are complex-valued and all wave modes have some level of spatial decay. The usual concept of band gap now has to be exchanged to that of a zone of strongly attenuated wave propagation, creating an obvious difficulty in determining the edge frequencies of a band gap. Several researchers have proposed alternatives. For example, Andreassen and Jensen (2013) and Chen et al. (2019) used the minimum imaginary component of all wave numbers at a given frequency, while Krushynska et al. (2016) utilized an effective loss factor. Collet et al. (2011) utilized an evanescence ratio index, which is the minimum imaginary component normalized by wave number absolute value. Pierce and Matlack (2021) developed an ingenious evanescence indicator for elastic metamaterials with one-dimensional periodicity that relates the decay component of the wave vector to the transmitted wave amplitude through a finite structure.

Since some level of damping is unavoidable in any real engineering structure, it is necessary to extend the current methodology of optimal design to damped elastic meta-structures, providing a deeper understanding of how damping may affect the desired performance. From the perspective presented herein, the main objective of this work is to obtain optimal band gaps in damped elastic meta-structures. Specifically, a modified objective function that incorporates an evanescence index integral is used to obtain optimal band gaps for the dissipative structure. The proposed methodology was applied to the damped counterpart of the resonant meta-structure considered by Salsa Jr et al. (2021) and the differences in methodologies with respect to optimizing a damped or undamped structure have been highlighted throughout the text. The unit cells under consideration were modeled by the finite element method and wave modes were obtained by taking into account Floquet-Bloch boundary conditions. While band gaps for the undamped structure can be identified by inspecting the associated dispersion relation, an evanescence index was used in the presence of damping. Furthermore, it is shown that the optimal damped structure has a wider range of attenuation than the undamped optimal one, but with decreased peak of attenuation. Finally, the methodology is validated for a finite structure, showing the optimized elastic metamaterial can decrease the transmissibility of mechanical waves over a wide range of frequencies, demonstrating its potential utility in diverse applications requiring vibration suppression.

METHODS

Model for a Three-dimensional Elastic Metamaterial

Salsa Jr et al. (2021) introduced the three-dimensional meta-structure shown in Fig. 1a. It consists of a cubic grid of size L, "outer" beam-like members, whose cross-sections are circular, with radius r_o. Additional beam-like struts are placed inside the cuboidal shape, so as to form a cross; these "inner" beams also have circular cross-section, with radius r_i. A solid sphere of radius r_e is added to the center of the unit cell. This unit cell is conceptualized in a manner so that the sphere and the inner beams can act as a local resonator. This structure can be used in architectural and mechanical fields for its high specific stiffness and large surface-to-volume ratio, while its band gap properties reveal potential applications in vibration isolation as support structures.

Since one-dimensional periodicity is common to many structures in engineering, it is assumed the infinite structure has translational periodicity along the z direction, as shown in Fig. 1b. Additionally, it is assumed that the infinite structure is slender, so that wave propagation is approximately one dimensional, i.e., it is assumed that waves propagate along the z direction. This hypothesis is not at all restrictive, since wave modes still involve the standard propagating and evanescent modes, related to longitudinal, bending, torsional and shearing motions.

The unit cell was modeled in ANSYS using a simplified finite element model. In this model, the structural frames were modeled according to Timoshenko beam theory using 540 BEAM188 elements from ANSYS library, which is capable of capturing shear-deformation effects. In addition, the central sphere was modeled as a rigid solid sphere connected to the inner beams but otherwise free to move, adding up to 6414 degrees of freedom for the unit cell model. Salsa Jr et al. (2021) showed dispersion relations obtained with this simplified model had good agreement with the ones obtained from a thee-dimensional model consisting of quadratic tetrahedral elements, with the advantage of lower computational cost. In

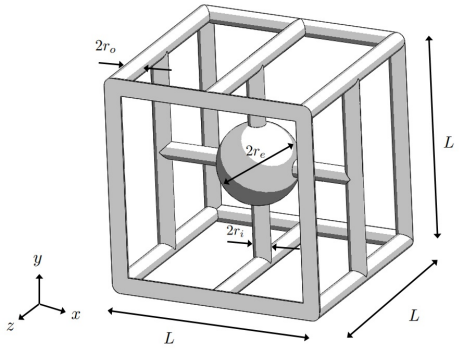

(a) Schematic of unit cell with resonator.

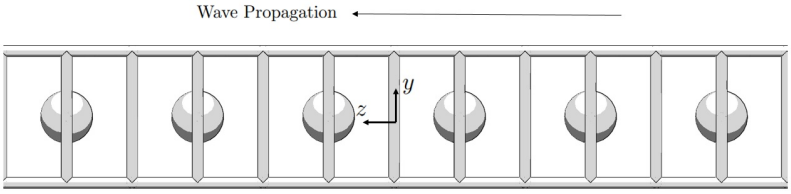

(b) One-dimensional wave propagation in the infinite structure. Waves may propagate to the left or right.

Figure 1: Unit cell of length L. Both outer and inner beams have circular cross-sections, with radii r_o and r_i, respectively. The sphere has radius r_e.

this work, it is assumed that structural damping is the main dissipation mechanism, but the methodology presented herein is applicable to systems subject to other forms of dissipation, such as viscous or viscoelastic damping, as well.

Computation of Band Structures

The wave modes of the considered meta-structure can be computed using the wave-based finite element method. This method is an attractive alternative when modeling complex structures, for which analytical solutions might not be readily available. In this manner, only the finite element model of a unit cell is needed, which is combined with Bloch's theorem and Floquet boundary conditions along the interfaces. Consequently, a hybrid approach, that involves computing the mass and stiffness matrices via commercial packages, can be seamlessly implemented (Nobrega et al., 2016). The method for one-dimensional periodic structures is concisely explained as follows. A finite element model of a unit cell is constructed and the mass and stiffness matrices are calculated. For consistency, each boundary along the direction of wave propagation must contain corresponding degrees of freedom. The dynamic equilibrium of a unit cell is formulated in terms of state vectors belonging to the left and right boundaries. Floquet periodicity along the propagation direction and application of Bloch's theorem result in the eigenvalue problem yielding information concerning the wave mode shapes, related to the spatial distribution of the displacements and internal forces over the cross-section of the unit cell along its boundaries, and wave numbers k.

Band gaps can be readily identified for the undamped structure: since k must be real for purely propagating waves, zones of attenuation can be detected from the dispersion relations $\mathbf{k}(\omega)$ at the frequency range where all wave numbers have non-zero imaginary part. In the case where dissipation is present, all wave numbers are complex and the situation is less clear. A method for identifying band gaps that renders itself useful for implementation in optimization routines involves the use of an indicator of minimal evanescence ratio of all computed waves for each considered frequency defined as (Collet et al., 2011)

$$\mathrm{Ind}(\omega) = \min_j \frac{|\Im[k_j(\omega)]|}{|k_j(\omega)|}, \tag{1}$$

where $\Im[k_j(\omega)]$ is the imaginary part of the j-th wave number, $k_j(\omega)$, and $|\cdot|$ represents an absolute value. To determine if $\mathrm{Ind}(\omega)$ represents a zone of strong attenuation (band gap) at ω, it is necessary to introduce a threshold value Ind_T: if

$\text{Ind}(\omega) > \text{Ind}_T$, then there is a band gap at ω. The specified value for Ind_T is arbitrary, and needs to be selected on a case by case basis, depending on the levels of damping and the structure under investigation.

Formulation of Optimization

Design Parameters

To obtain a band gap that is the widest and occurs at the lowest possible frequency range, geometric design parameters can be determined by formulating an appropriate optimization problem. For periodic structures, common strategies that have been used to achieve this desired goal involve variations of cross-sections in specific regions (Bibi et al., 2019; Dal Poggetto and Arruda, 2021; Dal Poggetto et al., 2021) and exploration of the effect of local resonance (Claeys et al., 2016; Miranda Jr. et al., 2019; Gao et al., 2019; Dal Poggetto et al., 2021). For these reasons, the design parameters chosen for band gap optimization are those directly linked with the internal oscillator, composed of the rigid sphere and internal elastic beams attached to the sphere. In particular, the radius of the internal beams, r_i, and the radius of the sphere, r_e, were considered as the two design variables. The radius of the sphere r_e impacts the mass of the local resonator and the radius of the internal beams r_i is a measure of the stiffness for the resonator. It should be noted that there is additional coupling between the radius of the sphere and the stiffness provided by the internal beams, since their length is directly impacted by the presence and size of the sphere.

In the optimization, the considered parameters are not entirely free to vary, being subjected to constraints. For simplicity, the radius of the internal beams r_i was restricted to lie in the range $r_i \in (0, r_o]$, where the upper limit r_o represents the radius of beams in the outer frame of the structure. In practice, the lower limit should be restricted to the minimal radius possible for additive manufacturing, if such structure was to be physically realized. The radius of the sphere can be restricted to lie in any range $r_e \in (0, R_{\max}]$, where $R_{\max} < L/2$, so that the sphere is always encased by the outer frame, and the lower limit characterizes a structure without a resonator.

Objective functions

When optimizing the undamped counterpart of the meta-structure in Fig. 1, Salsa Jr et al. (2021) achieved success by using an objective function that involves the ratio between the band gap mean frequency and its width:

$$\min_{r_i, r_e} f_{\text{obj}}^{(1)} = \min_{r_i, r_e} \frac{(\omega_u + \omega_l)/2}{(\omega_u - \omega_l)}, \tag{2}$$

where ω_l and ω_u are the lower and upper frequency limits of a band gap. The purpose of $f_{\text{obj}}^{(1)}$ is to maximize $\omega_u - \omega_l$ to obtain a band gap that is widest as possible, while at the same time minimizing its central frequency $(\omega_u + \omega_l)/2$. While this objective function is adequate to perform optimization of band gaps observed in undamped periodic structures, it needs to be slightly modified to accommodate systems with damping. This is necessary because application of (2) to a damped system may result in systems with larger attenuation zones, but whose intensity of attenuation might not be great enough to characterize a band gap. This issue can be circumvented by utilizing the modified objective function

$$\min_{r_i, r_e} f_{\text{obj}}^{(2)} = \min_{r_i, r_e} \frac{(\omega_u + \omega_l)/2}{(\omega_u - \omega_l) \int_{\omega_l}^{\omega_u} \text{Ind}(\omega) d\omega}. \tag{3}$$

Here,

$$\int_{\omega_l}^{\omega_u} \text{Ind}(\omega) d\omega \tag{4}$$

is the area of $\text{Ind}(\omega)$ in the interval (ω_u, ω_l). This simple adjustment guarantees that the attenuation in the interval (ω_u, ω_l) is significantly more intense than in other frequencies being considered. In should be reminded that, in this case, the band gap (ω_u, ω_l) is determined by the edge frequencies of the interval where the evanescence index (1) satisfies $\text{Ind}(\omega) > \text{Ind}_T$.

RESULTS

Initial Considerations

Before applying the optimization procedure, the unit cell was initially designed with the dimensions $L = 10$ mm, $r_o = 0.42$ mm, $r_i = 0.42$ mm and $r_e = 2$ mm. It is composed of structural steel, with density $\rho = 7850$ kg/m^3, Poisson

ratio $\nu = 0.3$, and Young's modulus $E = 200$ GPa. This material is chosen because of its immediate availability in finite element commercial packages, but the methodology presented herein is applicable to any chosen material. To accentuate any influence damping may have, a structural damping factor of $\eta = 1\%$ was utilized.

Salsa Jr et al. (2021) verified through dispersion curves that such initial design does not possess band gaps when damping is not considered. When dissipation is present, the wave numbers are still determined with the wave-based finite element method, but possible band gaps should be identified with the evanescence indicator in Eq. (1). Fig. 2a shows that waves are attenuated at all frequencies, but the initial design of the damped meta-structure has no zone of strong wave attenuation.

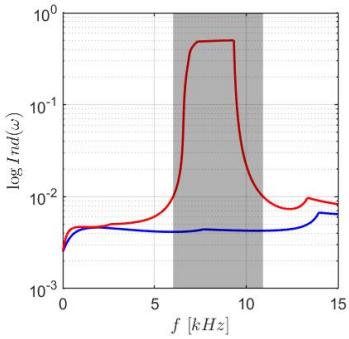

(a) Evanescence index for damped initial design (—) and optimal structure (—). Shaded region shows band gap.

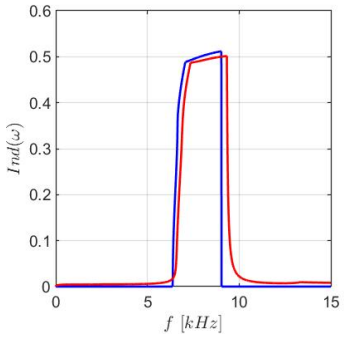

(b) Evanescence index for optimal solutions considering the undamped (—) and damped (—) cases.

Figure 2: Evanescence index.

Parametric Analysis of Band Gap Formation

When damping is included in the model, band gaps are not as easy to visualize because wave modes are attenuated at every frequency. In this case, a parametric analysis can be carried out utilizing the objective function (3). Fig. 3a shows how it varies when the radius of the sphere is assumed to be given by $r_e = 3.766$ mm, while r_i is varied in the range $(0,\ 0.42]$ mm. This upper limit is equal to the radius r_o of the outer beams. The constant value of r_e is arbitrarily chosen. Similarly, Fig. 3b shows how this objective function varies when the radius of the internal beams was held constant, $r_i = 0.145$ mm, while r_e was varied within the range $(0,\ 4]$ mm. Now, this upper limit is imposed as a size restriction, since the edges of the unit cell have length $L = 10$ mm. Fig. 3 shows that zones of intense attenuation can be created with larger values of r_e and an intermediate value of r_i. These trends follow what has been observed for the influences of r_e and r_i on the band gap formation when damping was not considered (Salsa Jr et al., 2021) — which makes sense, and should not be surprising.

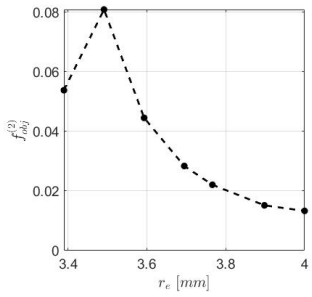

(a) Variation due to r_e when $r_i = 0.145$ mm.

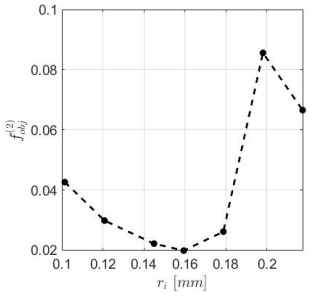

(b) Variation due to r_i when $r_e = 3.766$ mm.

Figure 3: Parametric analysis of the variation of $f_{\text{obj}}^{(2)}$ for the case of damped structure.

Optimizing the Resonator

Now, attention is directed to the minimization problem

$$\min_{r_e, r_i} f_{\text{obj}}^{(2)}. \tag{5}$$

During the optimization, the radius of the internal beams was restricted to lie in the range $r_i \in (0, 0.42]$ mm, where the upper limit 0.42 mm represents the radius of the outer beams. The radius of the sphere was restricted to lie in $r_e \in (0, 4]$ mm. The upper limit of 4 mm is due to size constraints, since the edges of the unit cell have length $L = 10$ mm.

This optimization was numerically solved using the differential evolution method, which has emerged as one of the most frequently used algorithms for solving complex optimization problems (Bilal et al., 2020). It is a meta-heuristic technique that follows the concepts of the theory of the evolution of species. Population generation is repeated until a termination criteria is met. If the optimization is carried in the frequency interval $[\omega_1, \omega_2]$, the termination criteria is that either $\omega_l = \omega_1$ and $\omega_u = \omega_2$, or that the best and worst solutions found in a population (determined by the values of $f_{\text{obj}}^{(2)}$) differ by $\Delta < 1\%$. The algorithm was initialized with $N = 20$ population members, and the frequency range analyzed was $0 - 10$ kHz, discretized in steps of 5 Hz. Due to the heuristic nature of the employed optimization methodology, 10 runs were performed, and the best solution among them (smallest value of $f_{\text{obj}}^{(2)}$) was taken to be the optimal one.

The main difference with respect to the optimization implemented by Salsa Jr et al. (2021) lies in the use of the evanescence index (1) and how to determine a band gap, since damping is now considered. As pointed out earlier, a threshold value Ind_T needs to be defined such that a band gap is present in the range (ω_l, ω_u) when $\text{Ind}(\omega) > \text{Ind}_T$. Since there is no universal way to determine Ind_T, it was found that

$$\text{Ind}_T = 2\% \cdot [\max_{\omega} \text{Ind}(\omega) - \min_{\omega} \text{Ind}(\omega)] \tag{6}$$

yielded satisfactory results for the meta-structure under consideration. The optimal values $r_i = 0.137$ mm and $r_e = 4$ mm were found when damping was taken into account for the unit cell dynamics. The optimization clearly generates a region of strong attenuation, as indicated by the shaded region in Fig. 2a. This region corresponds to a band gap defined by the threshold value (6).

It is interesting to note that the radius of the sphere is the same that was obtained in the undamped case by Salsa Jr et al. (2021). This happens because, in both cases, the sphere needs to be largest as possible to absorb lower frequency vibrations. On the other hand, the beam radius is approximately 1.04% greater than previously found for the undamped structure. Within engineering precision, these values are practically the same and it is possible to conclude that the structural damping incurred due to $\eta = 1\%$ had no effect on the optimal solution found for the investigated structure. However, even in this case, damping can have significant influence in the range and intensity of attenuation. As shown in Fig. 2b, no waves could propagate in the frequency range 6360-9006 Hz for the optimal undamped unit cell, whereas the zone of strong attenuation in the optimal damped structure comprises the frequency range 6020-10920 Hz. The addition of damping broadened the width of the band gap at the cost of a decreased peak of attenuation, a fact that has been observed by Van Belle et al. (2017) and Claeys et al. (2013) through case studies, but not by optimizing a damped structure.

Consideration of a Finite Structure

The results of the optimizations are now verified for a finite structure composed of 20 unit cells, such as the one shown in Fig. 4 (note that central spheres are not shown in the figure). It is expect that, as long as a sufficient number of unit cells are assembled, the finite structure can exhibit similar wave attenuation behavior to that found for the infinite periodic structure, at the cost that wave propagation is strongly attenuated but not completely forbidden inside a band gap (Pierce and Matlack, 2021).

No geometrical restrictions are imposed at this stage (free boundary conditions). Different harmonic base motions were imposed on the left interface of the structure, which is shaded in blue. Corresponding transmitted motion is calculated at the subsequent nodes, numbered 1-20. Nodes 1-19 (colored in black) are internal and node 20 (colored in red) is located at the right (free) interface. For example, if a base motion is imposed along y, then the y component of the displacement is measured for that point, and so on for x and z components. The torsional transmissibility, in particular, was calculated by imposing a rotation of the left interface about the z axis, and the corresponding rotation was measured for the indicated point at the right interface. This procedure was repeated four times, to account for the damped and undamped optimal structures with and without local resonator.

Fig. 5 compares the transmissibility of motions from node 0 across to the rightmost node 20 for the damped and undamped optimal cases. Figs. 5a, 5b and 5d indicate that bending and torsional modes have been significantly affected

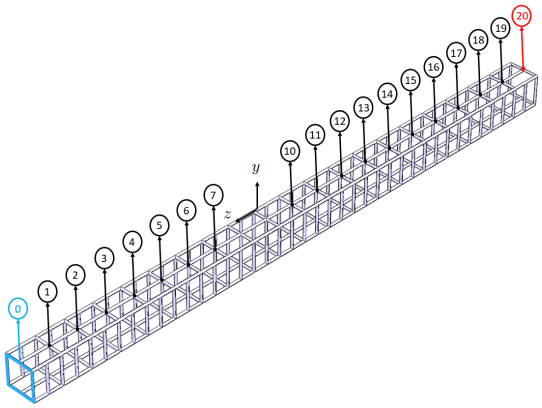

Figure 4: Finite structure with 20 unit cells with nodes 0-20. Numbering of nodes 8 and 9 as well as inner spheres have been omitted. The left interface, where base motions are applied, is colored in blue.

by the presence of damping, which broadened the width of the band gap and smoothed the peaks of attenuation. Curiously, Fig. 5c indicates the longitudinal mode is only slightly affected by the presence of damping.

A more complete picture of the finite meta-structures transmissibilities is provided by Fig. 6, when the displacements of all nodes are considered. For example, Figs. 6a-6h show the propagation of the four aforementioned types of motion along the optimal undamped and damped finite structures. In each graph, the amplitude ratio between nodes 1-20 and

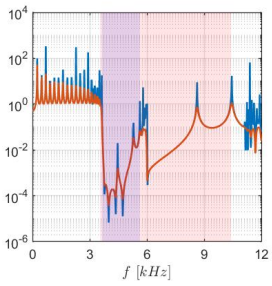

(a) Bending along y axis.

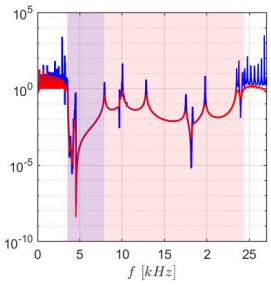

(b) Bending along x axis.

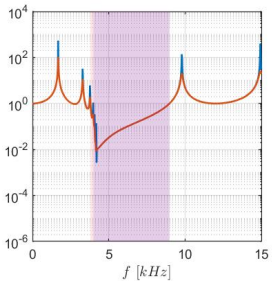

(c) Longitudinal motion.

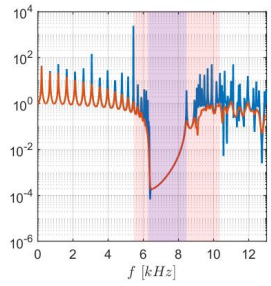

(d) Torsional motion.

Figure 5: Transmissibility of different displacement modes for undamped (—) and damped (—) finite meta-structures. The area shaded in light blue corresponds to the zone of attenuation for the undamped material, and light red shading to the damped one.

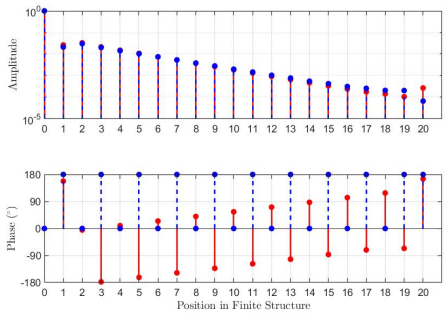

(a) Torsional motion for different nodes at 6400 Hz (inside band gap).

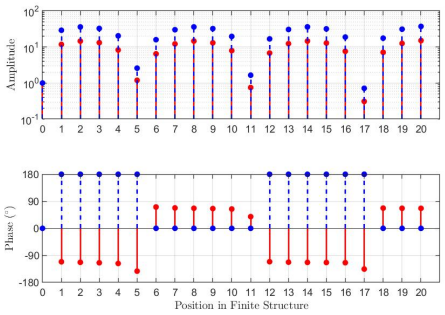

(b) Torsional motion for different nodes at 1666 Hz (outside band gap).

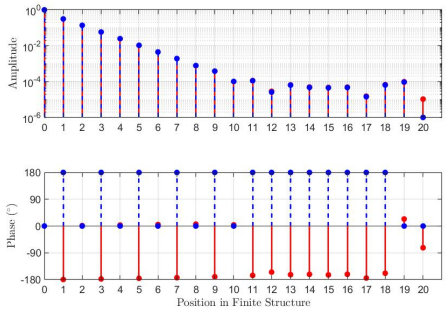

(c) Bending motion along x-axis for different nodes at 4080 Hz (inside band gap).

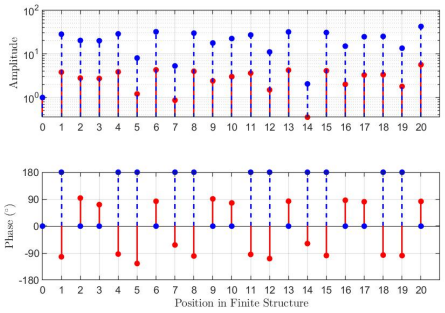

(d) Bending motion along x-axis for different nodes at 2516 Hz (outside band gap).

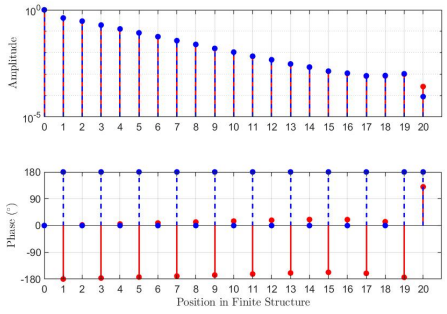

(e) Bending motion along y-axis for different nodes at 3780 Hz (inside band gap).

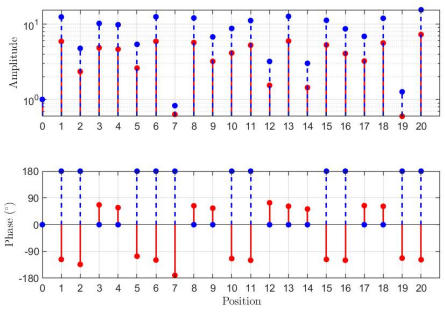

(f) Bending motion along y-axis for different nodes at 1833 Hz (outside band gap).

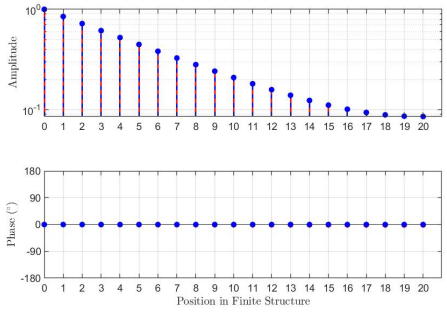

(g) Longitudinal motion for different nodes at 6000 Hz (inside band gap).

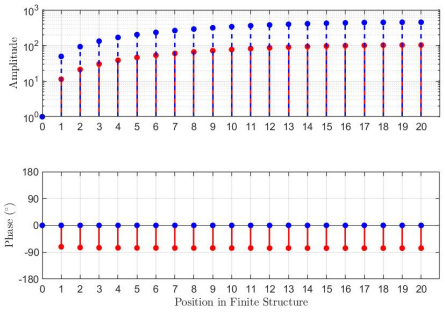

(h) Longitudinal motion for different nodes at 1683 Hz (outside band gap).

Figure 6: Amplitude ratio and phase of motion propagated across finite structure for undamped (- -) and damped (—) optimal solutions.

node 0 (where motion was inputted) are plotted, as well as the phase. In the case of the undamped material, the nodes are either in phase or 180° out of phase with respect to the imposed motion in node 0. At frequencies inside the zone of attenuation, motion decays spatially across the wave propagation direction for both cases. On the other hand, motion can be amplified at frequencies outside the zones of attenuation.

CONCLUSION

The localized resonators of a damped elastic meta-structure were successfully optimized by a differential evolution algorithm. The proposed modified objective function produced zones of strong attenuation in lower frequency ranges, which introduced decreased transmissibility of mechanical waves over a wide range of frequencies in a finite structure. This demonstrates the potential utility of the investigated elastic meta-structure in diverse applications requiring vibration suppression, specially when compared to its resonator-free counterpart.

ACKNOWLEDGMENTS

Authors would like to acknowledge the financial support provided by the São Paulo Research Foundation (FAPESP, grants #2018/15894-0 and #2020/06022-0). D.A. Rade acknowledges the Brazilian Research Council (CNPq) (grants #310633/2013-3 and #312068/2020-4).

REFERENCES

Andreassen, E. and Jensen, J.S., 2013. "Analysis of Phononic Bandgap Structures With Dissipation". Journal of Vibration and Acoustics, Vol. 135, No. 4. doi:10.1115/1.4023901.

Bacigalupo, A., Gnecco, G., Lepidi, M. and Gambarotta, L., 2017. "Optimal design of low-frequency band gaps in anti-tetrachiral lattice meta-materials". Composites Part B: Engineering, Vol. 115, pp. 341–359. doi:10.1016/j.compositesb.2016.09.062.

Bacigalupo, A., Gnecco, G., Lepidi, M. and Gambarotta, L., 2019. "Machine-learning techniques for the optimal design of acoustic metamaterials". Journal of Optimization Theory and Applications, pp. 1–24. doi:10.1007/s10957-019-01614-8.

Bibi, A., Liu, H., Xue, J.L., Fan, Y.X. and Tao, Z.Y., 2019. "Manipulation of the first stop band in periodically corrugated elastic layers via different profiles". Wave Motion, Vol. 88, pp. 205–213. doi:10.1016/j.wavemoti.2019.04.008.

Bilal, Pant, M., Zaheer, H., Garcia-Hernandez, L. and Abraham, A., 2020. "Differential evolution: a review of more than two decades of research". Engineering Applications of Artificial Intelligence, Vol. 90, p. 103479. doi:10.1016/j.engappai.2020.103479.

Chen, Y., Guo, D., Li, Y.F., Li, G. and Huang, X., 2019. "Maximizing wave attenuation in viscoelastic phononic crystals by topology optimization". Ultrasonics, Vol. 94, pp. 419–429. doi:10.1016/j.ultras.2018.05.005.

Claeys, C.C., Deckers, E., Pluymers, B. and Desmet, W., 2016. "A lightweight vibro-acoustic metamaterial demonstrator: Numerical and experimental investigation". Mechanical Systems and Signal Processing, Vol. 70-71, pp. 853–880. ISSN 0888-3270. doi:10.1016/j.ymssp.2015.08.029.

Claeys, C.C., Vergote, K., Sas, P. and Desmet, W., 2013. "On the potential of tuned resonators to obtain low-frequency vibrational stop bands in periodic panels". Journal of Sound and Vibration, Vol. 332, No. 6, pp. 1418–1436. doi:10.1016/j.jsv.2012.09.047.

Collet, M., Ouisse, M., Ruzzene, M. and Ichchou, M., 2011. "Floquet–bloch decomposition for the computation of dispersion of two-dimensional periodic, damped mechanical systems". International Journal of Solids and Structures, Vol. 48, No. 20, pp. 2837–2848. doi:10.1016/j.ijsolstr.2011.06.002.

Dal Poggetto, V.F., Bosia, F., Miniaci, M. and Pugno, N.M., 2021. "Optimization of spider web-inspired phononic crystals to achieve tailored dispersion for diverse objectives". Materials Design, Vol. 209, p. 109980. doi:10.1016/j.matdes.2021.109980.

Dal Poggetto, V.F. and Arruda, J.R.F., 2021. "Widening wave band gaps of periodic plates via shape optimization using spatial fourier coefficients". Mechanical Systems and Signal Processing, Vol. 147, p. 107098. doi:10.1016/j.ymssp.2020.107098.

Dal Poggetto, V.F., Serpa, A.L. and Arruda, J.R.d.F., 2019. "Optimization of local resonators for the reduction of lateral vibrations of a skyscraper". Journal of Sound and Vibration, Vol. 446, pp. 57–72. doi:10.1016/j.jsv.2019.01.017.

Gao, P., Climente, A., Sánchez-Dehesa, J. and Wu, L., 2019. "Single-phase metamaterial plates for broadband vibration suppression at low frequencies". Journal of Sound and Vibration, Vol. 444, pp. 108-126. doi: 10.1016/j.jsv.2018.12.022.

Jung, J., Goo, S. and Kook, J., 2020. "Design of a local resonator using topology optimization to tailor bandgaps in plate structures". Materials & Design, Vol. 191, p. 108627. doi:10.1016/j.matdes.2020.108627.

Krushynska, A., Kouznetsova, V. and Geers, M., 2016. "Visco-elastic effects on wave dispersion in three-phase acoustic metamaterials". Journal of the Mechanics and Physics of Solids, Vol. 96, pp. 29–47. doi:10.1016/j.jmps.2016.07.001.

Miranda Jr., E.J.P., Nobrega, E.D., Ferreira, A.H.R. and Dos Santos, J.M.C., 2019. "Flexural wave band gaps in a multi-resonator elastic metamaterial plate using kirchhoff-love theory". Mechanical Systems and Signal Processing, Vol. 116, pp. 480–504. doi:10.1016/j.ymssp.2018.06.059.

Nobrega, E.D., Gautier, F., Pelat, A. and Dos Santos, J.M.C., 2016. "Vibration band gaps for elastic metamaterial rods using wave finite element method". Mechanical Systems and Signal Processing, Vol. 79, pp. 192–202. doi:10.1016/j.ymssp.2016.02.059.

Pierce, C.D. and Matlack, K.H., 2021. "Fuzzy band gaps: a physically motivated indicator of bloch wave evanescence in phononic systems". Crystals, Vol. 11, No. 1. doi:10.3390/cryst11010066.

Salsa Jr, R.G., Sales, T.P. and Rade, D.A., 2021. "Optimization of vibration band gaps in three-dimensional lattice structures". In Proceedings of the 26th International Congress of Mechanical Engineering. ABCM. doi: 10.26678/ABCM.COBEM2021.COB2021-1019.

Van Belle, L., Claeys, C.C., Deckers, E. and Desmet, W., 2017. "On the impact of damping on the dispersion curves of a locally resonant metamaterial: Modelling and experimental validation". Journal of Sound and Vibration, Vol. 409, pp. 1–23. doi:10.1016/j.jsv.2017.07.045.

Vasileiadis, T., Varghese, J., Babacic, V., Gomis-Bresco, J., Navarro Urrios, D. and Graczykowski, B., 2021. "Progress and perspectives on phononic crystals". Journal of Applied Physics, Vol. 129, No. 16, p. 160901. doi:10.1063/5.0042337.

RESPONSIBILITY NOTICE

The author(s) is (are) the only party(ies) responsible for the printed material included in this paper.